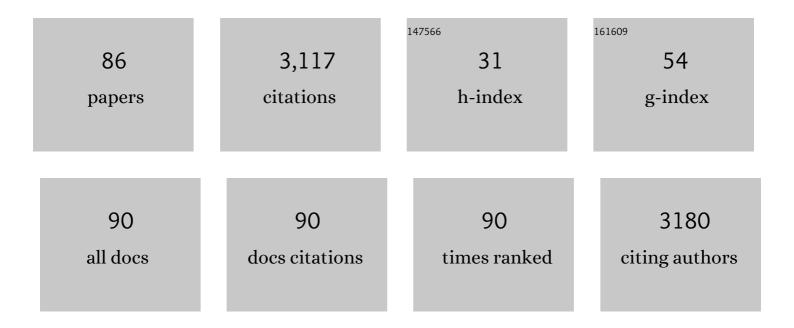
Ioannnis Papakonstantinou

List of Publications by Year in descending order

Source: https://exaly.com/author-pdf/2915956/publications.pdf Version: 2024-02-01



#	Article	IF	CITATIONS
1	A route to engineered high aspect-ratio silicon nanostructures through regenerative secondary mask lithography. Nanoscale, 2022, 14, 1847-1854.	2.8	7
2	Universal Theory of Light Scattering of Randomly Oriented Particles: A Fluctuational-Electrodynamics Approach for Light Transport Modeling in Disordered Nanostructures. ACS Photonics, 2022, 9, 672-681.	3.2	2
3	The impact of bead milling on the thermodynamics and kinetics of the structural phase transition of VO2 particulate materials and their potential for use in thermochromic glazing. Solar Energy Materials and Solar Cells, 2022, 242, 111783.	3.0	3
4	The Hidden Potential of Luminescent Solar Concentrators. Advanced Energy Materials, 2021, 11, 2002883.	10.2	102
5	Bandwidth limits of luminescent solar concentrators as detectors in free-space optical communication systems. Light: Science and Applications, 2021, 10, 3.	7.7	45
6	Optimization of the thermochromic glazing design for curtain wall buildings based on experimental measurements and dynamic simulation. Solar Energy, 2021, 216, 14-25.	2.9	23
7	Unique and universal dew-repellency of nanocones. Nature Communications, 2021, 12, 3458.	5.8	33
8	Precision-Microfabricated Fiber-Optic Probe for Intravascular Pressure and Temperature Sensing. IEEE Journal of Selected Topics in Quantum Electronics, 2021, 27, 1-12.	1.9	11
9	Delayed Lubricant Depletion of Slippery Liquid Infused Porous Surfaces Using Precision Nanostructures. Langmuir, 2021, 37, 10071-10078.	1.6	31
10	Bioinspired Multifunctional Glass Surfaces through Regenerative Secondary Mask Lithography. Advanced Materials, 2021, 33, e2102175.	11.1	13
11	Spacer-Defined Intrinsic Multiple Patterning. ACS Nano, 2020, 14, 12091-12100.	7.3	10
12	Thermoresponsive Black VO2–Carbon Nanotube Composite Coatings for Solar Energy Harvesting. ACS Applied Nano Materials, 2020, 3, 8848-8857.	2.4	8
13	Combined Effect of Temperature Induced Strain and Oxygen Vacancy on Metalâ€Insulator Transition of VO ₂ Colloidal Particles. Advanced Functional Materials, 2020, 30, 2005311.	7.8	42
14	Particle Size Evolution during the Synthesis of Gold Nanoparticles Using <i>In Situ</i> Time-Resolved UV–Vis Spectroscopy: An Experimental and Theoretical Study Unravelling the Effect of Adsorbed Gold Precursor Species. Journal of Physical Chemistry C, 2020, 124, 27662-27672.	1.5	11
15	Fluorine-Free Transparent Superhydrophobic Nanocomposite Coatings from Mesoporous Silica. Langmuir, 2020, 36, 13426-13438.	1.6	31
16	High-Performance Planar Thin Film Thermochromic Window via Dynamic Optical Impedance Matching. ACS Applied Materials & Interfaces, 2020, 12, 8140-8145.	4.0	22
17	All-Silicone-based Distributed Bragg Reflectors for Efficient Flexible Luminescent Solar Concentrators. Nano Energy, 2020, 70, 104507.	8.2	28
18	Influence of Lithium and Lanthanum Treatment on TiO 2 Nanofibers and Their Application in nâ€iâ€p Solar Cells. ChemElectroChem, 2019, 6, 3529-3529.	1.7	0

#	ARTICLE Herrischromic <mml:math.xmlns:mml="http: 1998="" math="" mathml"<="" th="" www.w3.org=""><th>IF</th><th>CITATIONS</th></mml:math.xmlns:mml="http:>	IF	CITATIONS
19	altimg="si1.svg"> <mml:mrow><mml:msub><mml:mrow><mml:mtext>VO</mml:mtext></mml:mrow><mml:mrov linebreak="goodbreak" linebreakstyle="after">â^^<mml:msub><mml:mrow><mml:mtext>SiO</mml:mtext></mml:mrow><mm nanocomposite smart window coatings with narrow phase transition hysteresis and transition</mm </mml:msub></mml:mrov </mml:msub></mml:mrow>		
20	gradient width. Solar Energy Materials and Solar Cells, 2019, 200, 109944. Origin of Performance Enhancement in TiO ₂ arbon Nanotube Composite Perovskite Solar Cells. Small Methods, 2019, 3, 1900164.	4.6	45
21	Atomic layer deposition of vanadium oxides: process and application review. Materials Today Chemistry, 2019, 12, 396-423.	1.7	46
22	Influence of Lithium and Lanthanum Treatment on TiO 2 Nanofibers and Their Application in nâ€iâ€p Solar Cells. ChemElectroChem, 2019, 6, 3590-3598.	1.7	5
23	All-Optical Rotational Ultrasound Imaging. Scientific Reports, 2019, 9, 5576.	1.6	47
24	Micron resolution, high-fidelity three-dimensional vascular optical imaging phantoms. Journal of Biomedical Optics, 2019, 24, 1.	1.4	7
25	Dynamically configurable, successively switchable multispectral plasmon-induced transparency. Optics Letters, 2019, 44, 3829.	1.7	5
26	Optical interferometric temperature sensors for intravascular blood flow measurements. , 2019, , .		3
27	The Effect of Alkali Metal (Na, K) Doping on Thermochromic Properties of VO2 Films. MRS Advances, 2018, 3, 1863-1869.	0.5	5
28	Polydimethylsiloxane Composites for Optical Ultrasound Generation and Multimodality Imaging. Advanced Functional Materials, 2018, 28, 1704919.	7.8	81
29	Improved thermochromic properties in bilayer films of VO ₂ with ZnO, SnO ₂ and WO ₃ coatings for energy efficient glazing. Journal of Materials Chemistry C, 2018, 6, 12555-12565.	2.7	22
30	Mitigation of hysteresis due to a pseudo-photochromic effect in thermochromic smart window coatings. Scientific Reports, 2018, 8, 13249.	1.6	11
31	TiO2 nanofiber photoelectrochemical cells loaded with sub-12Ânm AuNPs: Size dependent performance evaluation. Materials Today Energy, 2018, 9, 254-263.	2.5	23
32	A combined experimental and theoretical study into the performance of multilayer vanadium dioxide nanocomposites for energy saving applications. , 2018, , .		3
33	3D printed micro-scale fiber optic probe for intravascular pressure sensing. , 2018, , .		2
34	On the ability of Förster resonance energy transfer to enhance luminescent solar concentrator efficiency. Nano Energy, 2017, 32, 263-270.	8.2	60
35	Ultrasensitive plano-concave optical microresonators for ultrasound sensing. Nature Photonics, 2017, 11, 714-719.	15.6	255
36	Sensitive and specific detection of explosives in solution and vapour by surface-enhanced Raman spectroscopy on silver nanocubes. Nanoscale, 2017, 9, 16459-16466.	2.8	78

#	Article	IF	CITATIONS
37	Through-needle all-optical ultrasound imaging in vivo: a preclinical swine study. Light: Science and Applications, 2017, 6, e17103-e17103.	7.7	90
38	Optical fiber ultrasound transmitter with electrospun carbon nanotube-polymer composite. Applied Physics Letters, 2017, 110, 223701.	1.5	54
39	Impact of curvature on the optimal configuration of flexible luminescent solar concentrators. Optics Letters, 2017, 42, 2695.	1.7	14
40	Optical fiber laser ultrasound transmitter with electrospun composite for minimally invasive medical imaging. , 2017, , .		0
41	Large Scale Production of Photonic CrystalsÂonÂScintillators. IEEE Transactions on Nuclear Science, 2016, 63, 639-643.	1.2	7
42	Carbonâ€Nanotube–PDMS Composite Coatings on Optical Fibers for Allâ€Optical Ultrasound Imaging. Advanced Functional Materials, 2016, 26, 8390-8396.	7.8	120
43	Flexible and fluorophore-doped luminescent solar concentrators based on polydimethylsiloxane. Optics Letters, 2016, 41, 713.	1.7	27
44	Light Extraction From Scintillating Crystals Enhanced by Photonic Crystal Structures Patterned by Focused Ion Beam. IEEE Transactions on Nuclear Science, 2016, 63, 644-648.	1.2	6
45	Intelligent Multifunctional VO ₂ /SiO ₂ /TiO ₂ Coatings for Self-Cleaning, Energy-Saving Window Panels. Chemistry of Materials, 2016, 28, 1369-1376.	3.2	221
46	Losses in luminescent solar concentrators unveiled. Solar Energy Materials and Solar Cells, 2016, 144, 40-47.	3.0	82
47	Experimental Verification of Visible Light Communications based on Multi-Band CAP Modulation. , 2015, , .		13
48	Fundamental limits of concentration in luminescent solar concentrators revised: the effect of reabsorption and nonunity quantum yield. Optica, 2015, 2, 841.	4.8	38
49	Real-time needle guidance with photoacoustic and laser-generated ultrasound probes. Proceedings of SPIE, 2015, , .	0.8	4
50	Wavelength-Multiplexed Polymer LEDs: Towards 55 Mb/s Organic Visible Light Communications. IEEE Journal on Selected Areas in Communications, 2015, 33, 1819-1828.	9.7	51
51	A Multi-CAP Visible-Light Communications System With 4.85-b/s/Hz Spectral Efficiency. IEEE Journal on Selected Areas in Communications, 2015, 33, 1771-1779.	9.7	85
52	Multi-band carrier-less amplitude and phase modulation for bandlimited visible light communications systems. IEEE Wireless Communications, 2015, 22, 46-53.	6.6	68
53	Broadband miniature optical ultrasound probe for high resolution vascular tissue imaging. Biomedical Optics Express, 2015, 6, 1502.	1.5	99
54	Influence of Depth of Interaction upon the Performance of Scintillator Detectors. PLoS ONE, 2014, 9, e98177.	1.1	8

#	Article	IF	CITATIONS
55	Next Generation Visible Light Communications: 10 Mb/s with Polymer Light-Emitting Diodes. , 2014, , .		5
56	Highly sensitive optical microresonator sensors for photoacoustic imaging. Proceedings of SPIE, 2014, , .	0.8	3
57	Timing Performance Improvement of Scintillator Detectors via Inclusion of Reflection Metasurfaces. , 2014, , .		0
58	Laser-generated ultrasound with optical fibres using functionalised carbon nanotube composite coatings. Applied Physics Letters, 2014, 104, .	1.5	101
59	Homeotropic alignment and Förster resonance energy transfer: The way to a brighter luminescent solar concentrator. Journal of Applied Physics, 2014, 116, 173103.	1.1	31
60	Fiber optic ultrasound transducers with carbon/PDMS composite coatings. , 2014, , .		0
61	Visible light communications: real time 10 Mb/s link with a low bandwidth polymer light-emitting diode. Optics Express, 2014, 22, 2830.	1.7	73
62	Visible Light Communications: 170 Mb/s Using an Artificial Neural Network Equalizer in a Low Bandwidth White Light Configuration. Journal of Lightwave Technology, 2014, 32, 1807-1813.	2.7	109
63	Organic visible light communications: Recent progress. , 2014, , .		6
64	A 20-Mb/s VLC Link With a Polymer LED and a Multilayer Perceptron Equalizer. IEEE Photonics Technology Letters, 2014, 26, 1975-1978.	1.3	25
65	A 1-Mb/s Visible Light Communications Link With Low Bandwidth Organic Components. IEEE Photonics Technology Letters, 2014, 26, 1295-1298.	1.3	21
66	Component and System Level Studies of Radiation Damage Impact on Reflective Electroabsorption Modulators for Use in HL-LHC Data Transmission. IEEE Transactions on Nuclear Science, 2013, 60, 386-393.	1.2	1
67	Online artificial neural network equalization for a visible light communications system with an organic light emitting diode based transmitter. , 2013, , .		2
68	2.7 Mb/s With a 93-kHz White Organic Light Emitting Diode and Real Time ANN Equalizer. IEEE Photonics Technology Letters, 2013, 25, 1687-1690.	1.3	27
69	1.4-Mb/s White Organic LED Transmission System Using Discrete Multitone Modulation. IEEE Photonics Technology Letters, 2013, 25, 615-618.	1.3	34
70	A bioinspired solution for spectrally selective thermochromic VO_2 coated intelligent glazing. Optics Express, 2013, 21, A750.	1.7	90
71	Efficiency and loss mechanisms of plasmonic Luminescent Solar Concentrators. Optics Express, 2013, 21, A735.	1.7	28
72	Visible light communications: 375ÂMbits/s data rate with a 160ÂkHz bandwidth organic photodetector and artificial neural network equalization [Invited]. Photonics Research, 2013, 1, 65.	3.4	22

#	Article	IF	CITATIONS
73	A MIMO-ANN system for increasing data rates in organic visible light communications systems. , 2013, , .		21
74	FirstLight: Pluggable Optical Interconnect Technologies for Polymeric Electro-Optical Printed Circuit Boards in Data Centers. Journal of Lightwave Technology, 2012, 30, 3316-3329.	2.7	71
75	Exploiting Equalization Techniques for Improving Data Rates in Organic Optoelectronic Devices for Visible Light Communications. Journal of Lightwave Technology, 2012, 30, 3081-3088.	2.7	72
76	A Fully Bidirectional Optical Network With Latency Monitoring Capability for the Distribution of Timing-Trigger and Control Signals in High-Energy Physics Experiments. IEEE Transactions on Nuclear Science, 2011, 58, 1628-1640.	1.2	14
77	Integrated optical and electronic interconnect PCB manufacturing research. Circuit World, 2010, 36, 5-19.	0.7	40
78	Modal Dispersion Mitigation in Standard Single-Mode Fibers at 850 nm With Fiber Mode Filters. IEEE Photonics Technology Letters, 2010, 22, 1476-1478.	1.3	13
79	Passive Optical Networks for Timing-Trigger and Control applications in high energy physics experiments. , 2010, , .		0
80	Radiation- and Bound-Mode Propagation in Rectangular, Multimode Dielectric, Channel Waveguides With Sidewall Roughness. Journal of Lightwave Technology, 2009, 27, 4151-4163.	2.7	16
81	Insertion Loss and Misalignment Tolerance in Multimode Tapered Waveguide Bends. IEEE Photonics Technology Letters, 2008, 20, 1000-1002.	1.3	8
82	Low-Cost, Precision, Self-Alignment Technique for Coupling Laser and Photodiode Arrays to Polymer Waveguide Arrays on Multilayer PCBs. IEEE Transactions on Advanced Packaging, 2008, 31, 502-511.	1.7	43
83	Optical 8-channel, 10 Gb/s MT pluggable connector alignment technology for precision coupling of laser and photodiode arrays to polymer waveguide arrays for optical board-to-board interconnects. , 2008, , .		16
84	Innovative Optical and Electronic Interconnect Printed Circuit Board Manufacturing research. , 2008, , .		5
85	Integrated optical and electronic interconnect printed circuit board manufacturing. Circuit World, 2008, 34, 21-26.	0.7	10
86	Transition, radiation and propagation loss in polymer multimode waveguide bends. Optics Express, 2007, 15, 669.	1.7	62